Int. J. of Thermodynamics,
Vol. 8, (No. 2), pp. 103-113, June-2005

ISSN 1301-9724

Investigation of the Start-up Strategy for a Solid Oxide Fuel Cell Based Auxiliary Power Unit under Transient Conditions

Diego Rancruel and Michael von Spakovsky
Center for Energy Systems Research
Department of Mechanical Engineering
Virginia Polytechnic Institute and State University
Blacksburg, VA 24061
E-mail: drancrue@vt.edu, vonspako@vt.edu

Abstract

A typical approach to the synthesis/design optimization of energy systems is to only use steady state operation and high efficiency (or low total life cycle cost) at full load as the basis for the synthesis/design. Transient operation as reflected by changes in power demand, shut-down, and start-up are left as secondary tasks to be solved by system and control engineers once the synthesis/design is fixed. However, start-up and shut-down may be events that happen quite often and, thus, may be quite important in the creative process of developing the system. This is especially true for small power units used in transportation applications or for domestic energy supplies, where the load demand changes frequently and peaks in load of short duration are common. The duration of start-up is, of course, a major factor which must be considered since rapid system response is an important factor in determining the feasibility of solid oxide fuel cell (SOFC) based auxiliary power units (APUs). Start-up and shut-down may also significantly affect the life span of the system due to thermal stresses on all system components. Therefore, a proper balance must be struck between a fast response and the costs of owning and operating the system so that start-up or any other transient process can be accomplished in as short a time as possible yet with a minimum in fuel consumption.

In this research work we have been studying the effects of control laws and strategies and transients on system performance. The results presented in this paper are based on a set of transient models developed and implemented for the components of a 5 kWe net power SOFC based APU and for the high-fidelity system which results from their integration. The simulation results given below are for two different start-up approaches: one with steam recirculation and component pre-heating and the second without either. These start-up simulations were performed for fixed values of a number of system-level parameters (e.g., fuel utilization, steam-to-methane ratio, etc.) and were used to generate sufficient information to permit the development of appropriate control strategies for this critical operating point. These strategies are based on a balance between fuel consumption and response time. In addition, energy buffering hardware was added to the system configuration in order to minimize the effects of transients on fuel cell stack performance and lifetime.

Keywords: SOFC based APUs for stationary and transportation applications, start-up procedures, transient operation, synthesis/design and operational/control

1. Introduction

Currently, among all of the new and most promising technologies (under development) for energy conversion, low- and high-temperature fuel cells are leading candidates for stationary (distributed-power-generation) and transportation applications. Fuel cell systems (FCSs) are seen as more environmentally friendly and energy efficient than their primary fossil fuel counterparts and unlike renewable energy systems (with the exception of hydroelectric power) have a high potential for playing, in the

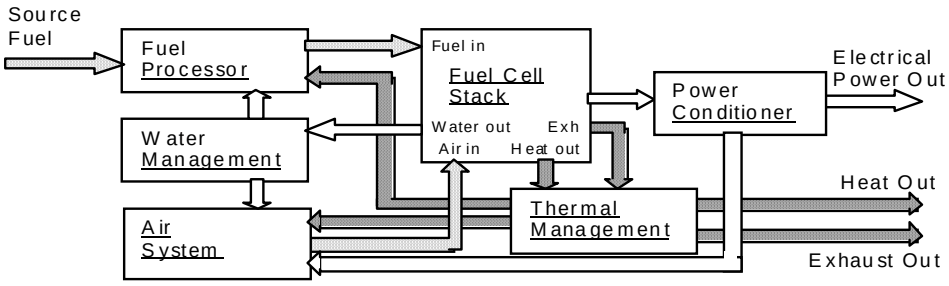

Figure 1. Fuel cell system (FCS) schematic

near- to mid-term, a significant role in the energy economy. One of the primary fuel-cell candidates for auxiliary power units are SOFC systems. Such systems typically consist of a fuel reformer (which in a transportation application may be on- or off-board); a fuel cell stack with appropriate water, air, and thermal management subsystems; power-electronics and power-conditioning subsystems; and some type of energy buffering for electricity, fuel, and air.

In a direct comparison of energy savings, fuel cell based power and cogeneration systems can exhibit a significant advantage over conventional systems, primarily due to their higher efficiencies at off-design conditions. Such significant energy gains as well as the nature of the fuel reforming process typical of these systems also lead to a considerable reduction in pollutants (CO_2, SO_2, NO_x, and CO emissions).

Of course, the gains both in terms of energy savings and pollutant emissions depend greatly on whether or not the fuel-cell system (as shown in *Figure 1*) is well synthesized and designed and whether or not appropriate control strategies have been developed to meet the varying load profiles for a variety of applications. In general, the SOFC stack, which comprises the stack subsystem (SS), responds quickly to changes in load because of rapid electrochemistry but is nonetheless limited by the stack's electrical responses, which are on the order of fractions of a second. This poses a problem in the SS's interaction with the power electronics subsystem (PES), which has an electrical response on the order of microseconds. In addition, response times for the thermal, mechanical, and chemical components in the balance of plant subsystem (BOPS) and particularly those for fuel processing (where load-following time constants are typically several orders of magnitude higher than those for the SS or the PES) handicap the FCS in quickly responding to changes in application load. Energy buffering can help mitigate this dichotomy in response times. Typically energy buffering is disregarded due to the capital cost increment. Therefore, differences in response times remain and manufacturers implement conservative schemes and additional hardware for managing stack responses to load variations (i.e. control tactics for delayed load-following to allow for BOPS response, expensive inductor filtering, etc.), making FCSs much less practical than they need to be from an application perspective.

One of the goals of the research on which this paper is based is the creation of tools that allow one to consider the applicability and effects on performance, response, and control of new system configurations, component designs, control architectures, and energy buffering. In Phases I and II of this work, comprehensive steady state and transient models were developed based on first principles and implemented using gPROMS® for each of the subsystems. Results for Phase I are found in Mazumder et al. (2003). In Phase II, a total life cycle cost optimization was performed applying original thermoeconomic based decomposition techniques and dynamically taking into account a mix of synthesis/design and operational/control decision variables for the BOPS/SS. Results for this dynamic optimization are found in Rancruel (2005) and Rancruel and von Spakovsky (2005). Parametric studies for the combined BOPS/SS/PES can be found in Mazumder et al. (2005, 2004) and Pradhan et al. (2005). Presented below are results for a parametric study of start-up procedures for the BOPS based on results initially presented in Rancruel and von Spakovsky (2004).

2. BOPS Modeling

PES response to changes in electrical loads depends on the response of the SS, which in turn depends on the BOPS response. Thus, steady and transient models of the BOPS must also be taken into account for accurate analysis of the overall FCS. A proposed BOPS super-configuration shown in *Figure 2* was conceived in our Phase I efforts in order to yield fast transient response times and maximum efficiency. The final optimal configuration determined during Phase II (see

Rancruel (2005) and Rancruel and von Spakovsky (2005)) is a varied subset of this super-configuration and is not presented here due to pending patent considerations. The start-up results presented below though applicable specifically to the configuration of *Figure 2* are, nonetheless, also applicable in general terms to the optimal configuration. Furthermore, the BOPS description, which follows, corresponds to both configurations, i.e. in its particulars to the super-configuration shown in *Figure 2* and in its generality to the optimal configuration not shown.

The BOPS consists of a fuel-processing subsystem (FPS) which converts natural gas to a hydrogen-rich reformate gas and a thermal management and power recovery subsystem to maintain fuel and oxidant temperatures and pressures at prescribed levels for the SOFC stack and provide energy for the fuel reforming. Note that some of the energy recovery is performed before the expansion process because of the high temperature energy recovery (higher than 800 K) required at the methane heat exchanger (HX III) and at the steam generator. The models developed for these subsystems can be used to analyze the thermodynamic, kinetic, and geometric characteristics of FCSs and their components at full and part loads.

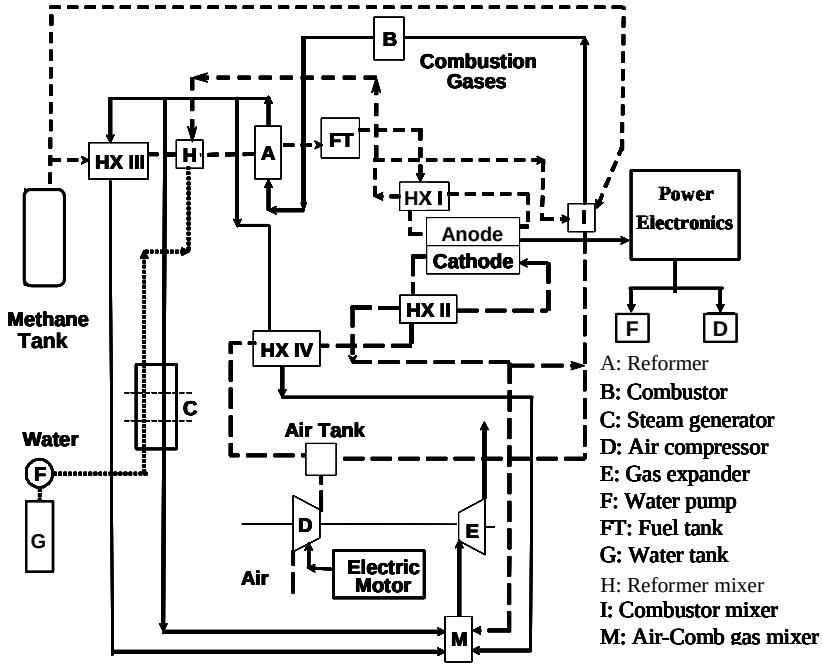

Figure 2. BOPS schematic.

2.1 Fuel processing subsystem (FPS)

The fuel feed for the FPS, which consists primarily of methane, comes from a high pressure storage tank. For stationary applications, the fuel may be supplied by either a pressurized tank or a commercial line. Regardless of the fuel supply system, the operational pressure in the reactor is never higher than 3 bars. After entering the system, a fraction of the fuel is supplied to the reforming line while the remaining fuel is used for combustion. The methane flowing down the reforming line is preheated by passing it through a compact, plate-fin type heat exchanger (HX III) and is then mixed with steam produced in a steam generator (C) in a reformer mixer (H) before entering the steam-methane reformer (A). The energy needed to drive the endothermic reforming reaction in the reformer is provided by the combustion gases leaving the combustor (B). The reformate gases coming out of the reformer are stored in a fuel tank (FT), which then acts as an energy buffer between the BOPS and the SS. This permits rapid supply of fuel to the SS when the stack demand is larger than the reformer production rate. One of the most important features of the proposed configuration is the recirculation of the anode products into the reformer mixer. The reactants coming out of the anode are rich in water vapor, which reduces the amount of new vapor required from the steam generator[1]. This in

[1] In fact, in the optimal configuration, the amount of water vapor available from recirculation during normal operation i.e. that not including start-up or shut-down, is such that the

turn yields a smaller steam generator and a smaller water tank (G).

2.2 Thermal management subsystem (TMS) and power recovery sub-system (PRS)

The combustion mixture, supplied to the combustor (B), consists of air taken from the air tank, a percentage of the hydrogen-depleted anode exhaust gas, and methane that bypasses the reforming line. Burning the residual hydrogen in the stack tail gas translates into a decreased consumption of additional methane in the burner and, therefore, to increased efficiency of the configuration. After providing the required thermal energy for the endothermic reforming reaction, the combustion gases are split into three streams, the first preheats the methane (HXIII), the second is passed through the steam generator where it supplies the necessary energy for producing the steam consumed in the reforming process, and the third is used to preheat the air flowing into the stack (HX IV). The mass flow of hot gases through these components is controled by the methane and steam water exit temperature from HX III and the steam generator. Finally, the combustion gas streams are mixed together before being expanded (E) and exhausted to the atmosphere.

In the BOPS and the SS, the temperatures of a number of critical components have to be carefully controlled and the flow and utilization of energy from several sources within the configuration have to be managed efficiently in order to achieve high overall efficiencies. Therefore, the TMS plays a significant role in the operation of the FCS. A number of high performance heat exchangers are used within the configuration in order to meet these objectives. Furthermore, since the SOFC operates at a high temperature, high-grade waste energy is used to precondition the streams coming into the stack while the stream coming out of the cathode, which is still rich in oxygen, is sent, for the most part, to the combustor mixer with only a fraction being sent to the expander. In addition, the exit temperature of the reformate gases and the rate of conversion at the reformer are controlled by the temperature and mass flow of the hot gases from the combustor. For fast response, a bigger mass flow of air in the combustor is required than that provided by the cathode. This extra air is taken from the air tank. In addition, energy recovery by flowing the mixed combustion gas stream mentioned above through an expander is used to offset some of the parasitic power requirements. For many operating conditions, the work produced by the expander does not quite match the work required by the compressor. This additional work is supplied by an electric motor which takes power from the SS/PES.

2.3 BOPS model description

The mathematical model of the BOPS consists of a set of equations for component and subsystem mass and energy conservation, kinetic behavior, and geometry. A detailed description of the Phases I and II equations for the BOPS components are found in Mazumder et al. (2003) and Rancruel (2005), respectively. Descriptions of the modeling approaches used for the principal components follow.

2.3.1 Modeling of the steam methane reformer

A number of simplifying assumptions are introduced to facilitate the modeling of the steam-methane reformer. The most significant are

- Reforming and combustion gases behave ideally in all sections of the reactor.
- The demethanation and water-gas shift reactions are considered to be kinetically controlled but are constrained by equilibrium considerations.
- Axial dispersion and radial gradients are negligible (plug flow conditions).

For the kinetic modeling, the rate equation developed by Bodrov, Apel'baum, and Temkin (1964) and Keiski et al. (1993) were selected to represent the demethanation and water-gas shift reaction rates, respectively. The reformate gas-side energy balance includes the gas sensible heat exchange, reaction enthalpies, heat exchange with the hotter tube-wall, heat exchange with the catalyst particles, and an accumulation or storage term. Mazunder et al. (2003) and Rancruel (2005) present a detailed explanation of the reformer kinetic model along with the energy balances of the reactor wall and the hot-side gases. TABLE I shows input parameter information for the reformer model.

2.3.2 Modeling of the compact heat exchangers

The heat exchangers used in the BOPS configuration are all plate-fin type, compact heat exchangers with a single-pass, cross-flow arrangement. Their modeling details are presented in Mazunder et al. (2003) and Rancruel (2005). The heat transfer and pressure drop models used are based on the work of Shah (1981) and Kays and London (1998). The expression for the heat exchanger effectiveness is

steam generator is not required (Rancruel (2005) and Rancruel and von Spakovsky (2005)).

obtained from Incropera and DeWitt (1990) and is valid for single-pass, cross-flow arrangements with both fluids unmixed. Since the fluid is a gas, its thermal capacitance is assumed to be small compared to the wall. In our research, a numerical approach was applied to solve the transient thermal response of the compact heat exchangers. In order to guarantee adequate accuracy, two-dimensional, spatial discretization was employed as well.

TABLE I. INPUT DATA FOR THE REFORMER SIMULATION.

Parameter	Value
Packing density in the reformer	1281.48 (kg/m^3)
Heat capacity of the catalyst	1.026 (kJ/kg-K)
Specific surface area of the catalyst	669.29 (m^2/m^3)
Arrhenius demethanation activation energy	83736 (J/mol)
Arrhenius demethanation frequency factor	0.0987 (kmol/kg h)
Steam to methane ratio	3.2
Number of finite difference sections in the reformer	20

2.3.3 Modeling of the steam generator

The steam generator consists of an economizer, an evaporator, and a superheater. These three integrated component parts were modeled as a counter-flow, shell-and-tube heat exchanger with a single-pass shell and one tube pass. Since the same type of shell-and-tube heat exchanger is taken into account to describe the economizer, evaporator, and superheater geometries, the geometric models developed are identical. The necessary equations are obtained from Kakaç and Liu (1998) and are the appropriate ones for this particular shell-and-tube configuration. The economizer, evaporator, and superheater dynamic models are formulated similarly. In general, the steam generator is discretized spatially into n sections. For each section (index i), a dynamic energy balance for the tubing is formulated. These energy balances are similar to the ones presented for the compact heat exchangers.

2.3.4 Modeling of the air compressors and the expander

For the dynamic analysis of a compressor or fan, the pressure ratio and reduced mass flow are state variables. Assuming that the inlet temperature is known, performance maps can then be used to calculate the required rotational speed and efficiency which in turn are used to determine the output temperature and work input. Heat transfer from the fluid in a compressor to the impeller and casing is a complex phenomenon, particularly during start-up transients. Heat flows from the fluid to the casing to the ambient as well as from the fluid to the impeller to the casing to the ambient through the bearings, seals, and shaft. The thermal capacitance of the casing, impeller, and inlet duct can be approximated by a single thermal mode at a particular temperature. A similar approach is used for the expander.

The work required by the compressor is determined from a mechanical energy balance. The shaft component is used to compute the turbo-machinery rotational speed based on input values of turbine power output and compressor power input.

3. BOPS Control

3.1 Control parameter and control variable set definitions

A set of system-level control variables have been defined, whose purpose is to keep the component-level dependent variables within acceptable ranges, which in turn can be initially defined as component control limits (e.g., such as maximum stack inlet temperature) or as the output of a trade-off or optimization process (e.g., reformer optimum operating temperature).

The system-level control variables chosen[2] for the BOPS are the steam-to-methane ratio (SMR), the fuel utilization (FU), the air-to-fuel ratio (AFR), and the fuel reformate ratio (FRR). The steam-to-methane ratio allows control of the chemical reaction inside the steam reformer. The fuel utilization affects BOPS energy recovery (in the form of heat and work interactions) and is important for characterizing the reaction in the stack. The air-to-fuel ratio is the ratio between the air and fuel going to the combustor. It affects the parasitic power requirements and the mass flow and temperature of the combustion gases exiting the combustor as well. Finally, the fuel reformate ratio is the ratio between the methane used in the reformer and the methane burned in the combustor. It permits control of the outlet temperature of the steam-methane reformer. In addition, the proportions into which the stream of

[2] Note that the term “control variable” is used here in the sense of a thermodynamic operational decision variable and not in the strict sense of what is directly or physically controlled within the system. For example, physically, there is no such thing as a FU (fuel utilization) controller. Instead, a mass flow rate controller of fuel to the stack for a given current density and load controls the FU. Thus, FU as a control variable has a mathematical sense (i.e. it is an independent variable) but not a physical one.

hot gases leaving the reformer is divided (one stream to the steam generator and two to two separate compact heat exchangers) can be used as a system-level control parameter as can the air stoichiometric ratio in the stack.

3.2 Fuel and energy buffering

The time response dichotomy mentioned above can diminish the performance of SOFC electrodes with increasing load as can current and voltage ripples which result from particular PES topologies and operation. Thus, ripples, load changes, and differences in transient response must be approached in a way which ensures not only that efficiency and power density, fuel utilization, and fuel conversion are optimal at all loads but that system response and reliability are maintained at optimal levels for all operating conditions. This can be aided by introducing fuel, air, and electrical energy buffering into the system layout.

As can be seen in *Figure 2* above, such buffering has been added to the system configuration. Typically buffering is only used in stationary systems because of the additional weight and volume, which for transportation systems is an operational penalty. However, in this work, the air and fuel tanks considered are very small and light (initial tank designs have yielded 1 liter volumes). It is important to note that the tanks are used to minimize transient effects, to increase response capabilities, and to minimize the subsystem interaction effects during transients. They are not intended for long term storage. With this in mind, it is reasonable to explore a trade-off between the advantages of using buffering devices and the penalties for using them.

The control strategy developed for the BOPS ensures that the fuel and the air in the tanks are never depleted. In addition, during load transients, the load on the SOFC, which is not a stiff voltage source and is, thus, connected to the load through the PES, is met by the batteries until the BOPS is able to supply fuel at the required rates. However, because the batteries (depending on their size) discharge at relatively rapid rates, their duration of operation is relatively small and must, therefore, be combined with a pressurized fuel tank which can rapidly supply fuel to the stack. In addition for transportation applications, the intention is to use the actual battery set of the vehicle instead of a separate battery bank. For stationary applications, batteries can be replaced by the grid if present.

4. Control Laws and Strategies

Figure 3 shows the proposed control scheme for the BOPS integrated with the PES and SS. A multi-level control approach is used in order to help improve the time response of the BOPS. The first level is determined by the air and fuel tank pressures. The objective of the fuel processing and air supply subsystems is to keep the tank pressure at fixed values. Disturbances in tank pressures appear as the fuel and air stack requirements change. Control strategies should guarantee that the fuel in the tank is never depleted and should ensure that no shut-down process is complete before proper levels of fuel in the tank are reached. Two additional control actions are implemented for the steam methane reformer with the objective of regulating the reformate gases exit composition and temperature. At the steam-methane reformer, the reformate gases temperature and composition are controlled using the hot gases inlet temperature and mass flow, respectively, as control variables. The pairing of the state variables and control variables was determined using the relative gain array matrix approach (i.e. a common technique of control theory).

The second level of control is defined by the hydrogen and air stack requirements. As the load changes, the amount of hydrogen out of the tank is changed by regulating the flow valve. The air tank valve is regulated to maintain the proper stoichiometric ratio in the stack.

The third level of control is defined by the rate change in load demand and battery bank charge level. For sudden changes in load, the difference between the produced and required power is supplied by the battery bank. The power required to keep the charge level is considered a parasitic power. Finally, for small increments in power demand, the system is able to assure direct stack response until proper hydrogen mass flow is reached. This is done by increasing the fuel utilization up to safe levels. Reductions in power demand are easier to control, since these can be done by reducing fuel utilization; reducing hydrogen mass flow; and by switching the battery bank to charge mode. Further details of the complete and optimized control strategy developed is found in Ran-cruel (2005) and Rancruel and von Spakovsky (2005).

4.1 Start-up strategy with battery bank

An analysis of the proposed con-figuration and control strate-gies and a consideration of the need for a fast response to load changes lead to the following system start-up control strategy:

1. First the turbo-machinery is started. At this point energy is taken from the battery bank.
2. Once the turbo-machinery is operating, the TMS starts. Fuel and air is delivered to the combustor and hot combustion gases are produced in order to generate steam and heat up the system components.

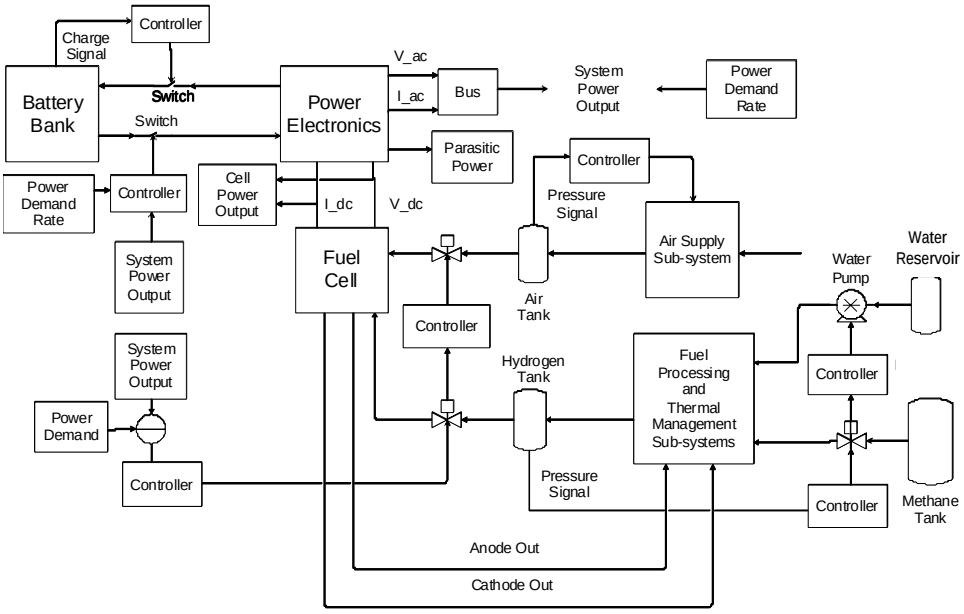

Figure 3. Multi-level control subsystem

3. Once the heat source is available, the steam generation process starts. The hot gas mass flow through the steam generator during start-up is higher than at the design point. This is done in order to speed up the convergence to steady state at high vapor temperatures. The water coming out of the steam generator is recirculated. Thus, no water is wasted and the inlet temperature is increased.

4.1 While adequate vapor temperatures are being reached, hot combustion gases are used for thermal conditioning of heat transfer devices. Thus, hot gases are passed through the hot-side of the system's heat exchangers and reformer. Hot gas flow through components is constrained by temperature gradient limits.

4.2 At the same time, the SOFC stack is conditioned for high temperature operation.

5.1 The streams of hot gases coming out of the TMS are mixed together. If the output temperature is high enough, the PRS starts: the expander is coupled to the air compressor (screw-type arrangement).

5.2 The SOFC stack starts using reformate fuel and air from the high pressure tanks: SOFC electrical energy generation commences.

5.3 The SOFC and the PES are coupled in order to start the generation of alternating current.

6. The turbo-machinery stops taking energy from the battery bank, which begins to be recharged.

7.1 With the FPS components and steam at operational temperatures, the steam generator recirculation stops and the fuel processing begins.

7.2 The FPS and the SOFC stack are coupled through the high pressure fuel tank. A minimum level of mass in the tank is required at all times.

8. The FPS and air compressor are never shut-down until proper levels in the air and fuel tanks are reached.

5. Results

For start-up, the BOPS was first analyzed at the component level. Before the production of hydrogen starts at the reformer, it is necessary to generate steam at temperatures above 800 K. To reach these conditions as soon as possible while assuring material integrity, the temperature and mass flow of the hot gases are controlled. The higher the gas inlet conditions, the faster the steam reaches operational conditions.

To reach these conditions, one of two procedures can be followed. In the first approach, both cold water and hot gases are passed through the steam generator; and until operational conditions are reached, the water coming out of the steam generator is recirculated to the water tank. Two advantages result from this approach. No water is wasted, and the water inlet temperature increases with time, which increases the rate at which the metal heats up. *Figure 4* shows the spatial and temporal thermal responses of steam generator start-up on the water side. It

can be seen how water exit temperatures higher than 800 K are reached in about 300 s while steady state is reached in 600 s.

In the second approach, the water coming out of the steam generator is recirculated directly back into the steam generator. Again, this approach results in no water being wasted and the water inlet temperature increases with time, however, at a much higher rate than with the first approach. *Figure 5* shows a comparison between the transient responses for the two approaches. For the case with direct recirculation to the steam generator, the water takes 195 s to reach 850 K. Note how immediately after stopping the direct recirculation (at 200 s), the steam temperature is above 850 K and is ready to be used in the reformer. In the case with tank recirculation, it takes the steam 300 s to reach temperatures above 800 K. In both cases, the rate of temperature increase of the steam reformer walls and the water stream depends on the mass flow and temperature of the hot gases and on the mass of the steam generator.

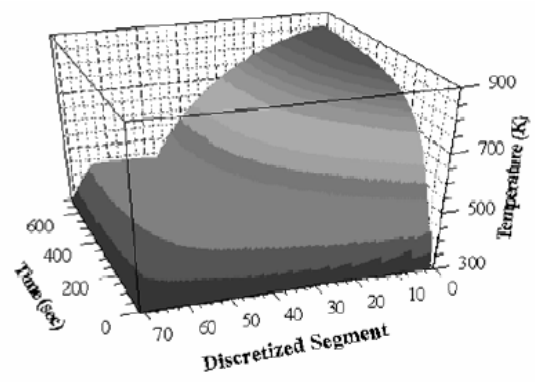

Figure 4. Steam generator start-up temporal and spatial thermal responses on the water side

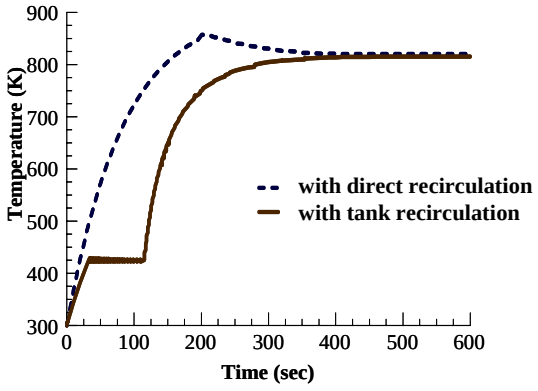

Figure 5. Steam generator start-up comparison of thermal responses on the water side

During transient operation, especially at start-up and shut-down, material resistance to thermal stresses were taken into account in order to assure the integrity of all components. This was controlled by introducing temperature gradient and heat flux constraints into the dynamic synthesis/design and operational/control problem. For the present study, it was found that the heat flux occurring throughout the steam generator during start-up is never more than 150 kW/m^2, which is significantly less than the maximum allowable value (burnout flux) of 340 kW/m^2.

Figure 6 shows the spatial and temporal performance of the steam-methane reactor during start-up. Notice that the plot starts at 200 s, which is the time that it takes for the steam generator to start up and at which point the recirculation is stopped. During recirculation, all thermal components are pre-heated. This means that hot gases are passed through these components without any cold-side flow. The final conditions (metal temperature) after the pre-heating period depend on the mass flow and temperature of the hot gases and on the mass of the component. Again, temperature gradients must be taken into account. To generate Figure 6, an initial synthesis/design point mass flow of hot gases was used during pre-heating (0.000503 kmol/s). It took the reformer 410 s to reach steady state at a maximum methane conversion rate of 90%. Without pre-heating, steady state is reached in 1050 s. The duration of the transient depends on the degree of pre-heating and the mass flow conditions on both sides of the reactor. Notice that the initial conversion rate at the reformer exit may not be zero if the pre-heating is high enough.

Figure 7 shows the reformer wall temperature response during start-up. The first 200 s corresponds to the preheating period. Initially, the temperature of the metal starts increasing at a higher rate on the hot-gas inlet side. At the end of the pre-heating period, the temperature of the metal close to the hot-gas inlet side (position ratio 10.0 at 200 s) is slightly higher than the steady state temperature; and the temperature of the metal close to the reformate-gas inlet side (position ratio 0.0 at 200 s) is lower than the steady state temperature. This behavior produces higher thermal stress in the axial direction than those present during steady state operation. Thus, for start-up, both control variables and physical limits or constraints should be taken into account during the synthesis/design process.

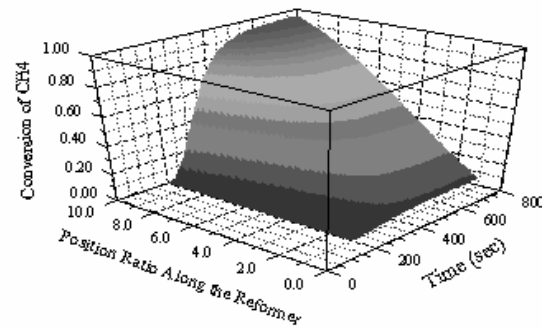

Figure 6. Steam-methane reformer start-up dyna-mic response for high pre-heating.

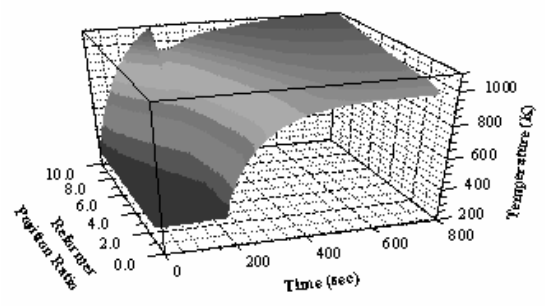

Figure 7.Steam methane reformer wall temperature start-up response for high pre-heating.

A comparison between the thermal responses of heat exchanger III for the cases with and without pre-heating is shown in Figure 8. Again, the pre-heating time is 200 s. When pre-heating finishes and cold-side flow starts, conditions are such that the cold stream exit temperature is at operational conditions. If no pre-heating is used, 195 additional seconds are required to reach operational conditions. Furthermore, the heat exchanger model uses a two-dimensional grid of 400 discrete elements, which allows a detailed and fairly accurate prediction of the temperature distribution in each compact heat exchanger. *Figure 9* shows this two-dimensional temperature distribution on the cold side for heat exchanger III. The y and x axes are scaled on the basis of the number of discrete segments in each direction.

Figure 10 shows the reformer fuel tank pressure response for a non-optimized PID controller responding to a decrease in load demand starting from full load. The change in load demand induces a change in hydrogen demand from the fuel tank. In the cases plotted in *Figure 10*, the load demand decreases, thus, reducing the required hydrogen from the fuel tank. This causes the tank pressure to increase. Even though the pressure in the tank takes about 1300 s to stabilize at a final value, the controller is able to keep the error below 2% even for the largest possible load change (80%). Also note that the larger the perturbation in load, the larger the maximum error in tank pressure is. Faster pressure controllers are possible to implement and were in fact modeled. However, it was observed that decreasing the pressure response time increases perturbations in methane conversion, since this increases the rate at which the reformate flow through the reformer changes. This is an illustration of how much coupled the system is.

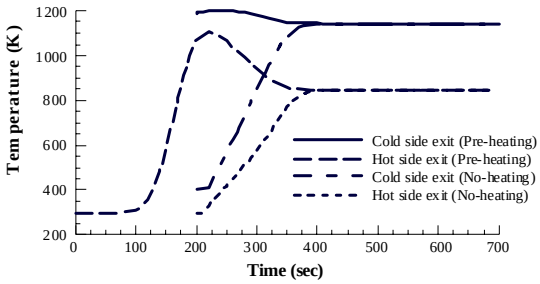

Figure 8. Compact heat exchanger III start-up thermal time response comparison between pre-heating and no pre-heating.

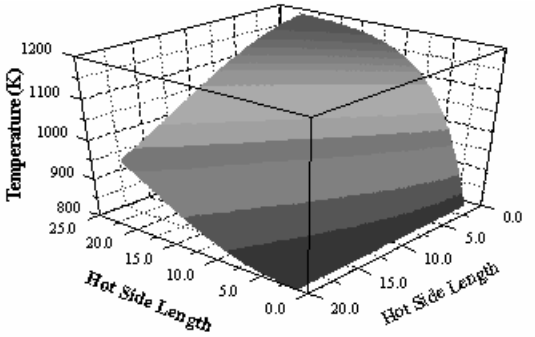

Figure 9. Compact heat exchanger III 2D spatial temperature distribution at steady state for the cold-side stream.

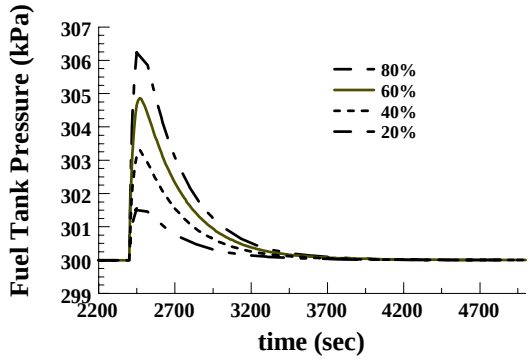

Figure 10. Fuel tank pressure transient with PID controller for decreasing changes in load demand starting from full load.

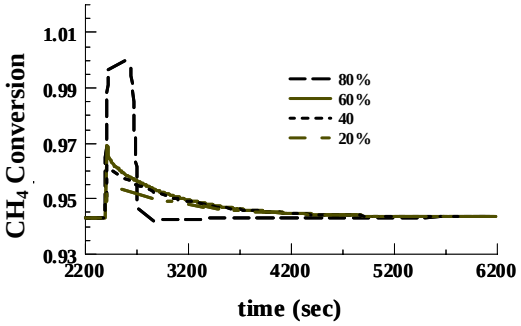

Figure 11. Methane conversion transient with PID controller for decreasing changes in load demand starting from full load.

Figure 11 shows the methane conversion control at the reformer for a set of non-optimized PID controllers[3] for decreasing load demand starting from full load. After a decrease in load occurs, a spike in the conversion rate results for all cases of load change due to a reduction in reactant flows. The size of the spike depends on the size of the load perturbation. The spike reveals how the energy stored in the reactor walls and catalyst affects the dynamic response. The higher the load perturbation, the bigger the conversion spikes are. For the case of 80% load demand perturbation, the induced change in reactant flows leads to a peak of almost 100% conversion. Note how the controller reaches steady state faster for the 80% perturbation. However, the maximum error is also the highest for this case. On the other hand, for the other cases, the response is slower, but the maximum error is reduced. This feature points to the possible need for a non-linear controller or the use of a variable gain array matrix to increase the controller gain for moderate and small changes in load.

6. Conclusions

The U.S. DOE project ("An Investigation to Resolve the Interaction between Fuel Cell, Power Conditioning System, and Application Loads," Cooperative Agreement Number: DE-FC26-02NT41574) on which this paper is based directly addresses several key technical issues for SOFC based APU development: (a) cost, (b) energy efficiency and power density, and (c) SOFC stack durability and reliability. To deal with these, modeling and simulation solutions and software codes/tools are needed which enable rapid syntheses/designs of a wide range of SOFC based power systems and APUs in a virtual environment which minimizes the actual costs and times for development. Towards that end, a virtual prototype, based on comprehensive and high-fidelity models of the SS, BOPS, PES, and application loads have been developed to determine potential component and system synthesis/design problems; to analyze interactions among the various subsystems and application loads on a system as well as a detailed-component level (e.g., component geometries in general and the internal dynamics and properties of SOFC stacks in particular) during steady-state, transient, and rapid start-up/shut-down conditions; to investigate component electrical and thermal behavior as well as the design of control subsystem architectures; and to conduct analyses, investigations, and predictions using mathematical optimization and/or trade-off studies. This paper has presented some detailed initial results pertinent to BOPS/SS dynamic synthesis, design, operation and control. For more results, the interested reader is referred to Mazunder et al. (2003), Rancruel (2005), and Rancruel and von Spakovsky (2005).

As to the most significant results presented in this paper, the control law for the FPS has a multi-level feedback with the primary level determined by the level in the pressurized fuel and air tanks, the secondary level by the consumption rate of hydrogen in the SOFC stack, and the third level by the rate of load change. The control law for the stack is defined by safe operating conditions (fuel utilization and stack temperature gradients) and power requirements. The control strategy, which has been developed in this work, is constrained by these laws and is suitable for meeting the stringent transient conditions which the system must undergo, especially at start-up. This strategy must offer adequate time responses to sudden and large changes in power demand, while fuel and energy buffering devices added to the system configuration significantly speed up system response to any type of load perturbation. As a initial step, multiple model based PID controllers were implemented to control system operation. The inputs and outputs were selected and matched using the relative gain array (RGA) approach. Adaptive and predictive capabilities were considered in order to manage the wide range of operational conditions and transient events. More details about our efforts in this area are given in Rancruel (2005), and Rancruel and von Spakovsky (2005).

[3] The results for the "non-optimized" controllers presented throughout this paper are a result of initial parametric studies done during Phase I and the initial part of Phase II of our research work. Since then a set of "optimized" controllers resulting directly form the dynamic synthesis/design and operational/control optimization of the coupled BOPS/SS have been determined. Results for these controllers can be found in Rancruel (2005) and Rancruel and von Spakovsky (2005).

Finally, the steam reformer was designed to generate vapor at operational conditions for maximum demand within 200 s without risk of damage due to temperature gradients. During this time, a pre-heating strategy was implemented. Pre-heating reduced the start-up time of the reformer (the slowest component) by about 640 s. This was done while assuring the physical integrity of the component. The fuel tank assures 560 s of fuel supply to the fuel cell stack at maximum power demand. By using pre-heating, the heat exchangers are assured of being at operational conditions the moment the steam generator starts providing vapor to the reformer.

Acknowledgement and Disclaimer

The authors would like to thank the U.S. Department of Energy (DOE) for the financial support (Cooperative Agreement Number: DE-FC26-02NT41574) which has made possible the work on which this paper is based. However, the U.S. DOE makes no warrantee of the accuracy, completeness, or usefulness of any of the information presented in this paper. Furthermore, the views and opinions expressed by the authors do not necessarily state or reflect those of the United States government or any agency thereof.

References

Bodrov, N. M., Apel'baum, L. O., and Tem-kin, M. I., 1964, in Murray, A. P. and Snyder, T. S. (Editors), "Steam-Methane Reformer Kinetic Computer Model with Heat Transfer and Geometry Options", *Industrial Engineering Chemical Process Design and Development*, Vol. 24, No. 2, p. 289.

Incropera, F. P., and DeWitt, D. P., 1990, *Fundamentals of Heat and Mass Transfer*, 3rd edition, John Wiley and Sons, Inc., New York.

Kakaç, S. and Liu, H., 1998, Heat exchangers: Selection, Rating, and Thermal Design, CRC Press, Boca Raton, Florida.

Kays, W. M. and London, A. L., 1998, Com-pact Heat Exchangers, Krieger Publishing Co., Malabar, FL.

Keiski, R. L., Desponds, O., Chang, Y. –F., and Somorjai, G. A., 1993, "Kinetics of the Wa-ter-Gas Shift Reaction over Several Alkane Activation and Water-Gas Shift Catalysts", *Applied Catalysis A*, Vol. 101, No. 2, pp. 317-338, Aug.

Mazumder, S. K., Acharya K., Burra R., Haynes C., Willian R., von Spakovsky M. R., Rancruel D. F., Nelson D., Hertvigsen J., Elangovan S., Mckintyre, C., Herbison D., 2003, "An Investigation to Resolve the Interaction Between Fuel Cell, Power Conditioning System And Application Loads". Topical report, U.S. Department of Energy, Cooperative Agreement Number: DE-FC26-02NT41574, October.

Mazumder, S.K., Pradhan, S, Hartvigsen, J., von Spakovsky, M. R., Rancruel, D., 2005, "Effects of Battery Buffering and Inverter Modu-lation on the Post Load-Transient Performance of a Planar Solid-Oxide Fuel Cell," *IEEE Transac-tions on Energy Conversion*, IEEE, in press.

Mazumder, S.K., von Spakovsky, M.R., Haynes, C., Acharya, K., Rancruel, D., Williams, R., Nelson, D., Gemmen, R.S., Hertvigsen, J., 2004, "Solid-Oxide-Fuel-Cell Performance and Durability: Resolution of the Effects of Power-Conditioning Systems and Application Loads," *IEEE Transactions*, IEEE Power Electronics Society, vol. 4, no. 5, pp 1263-1278, September.

Pradhan, S, Mazumder, S.K., Rancruel, D., von Spakovsky, M.R., Hollist, M., Hartvigsen, J., Kahleel, M., 2005, "A Modeling Framework for Planar Solid Oxide Fuel Cell based Power Conditioning System for Vehicular APUs," *IEEE Transactions*, IEEE Power Electronics Society, special issue on Automotive Power Electronics & Motor Drives, in press.

Rancruel, D. F., 2005, "Dynamic Synthesis/Design and Operation/Control Optimization Approach Applied to a Solid Oxide Fuel Cell based Auxiliary Power Unit under Transient Conditions," Ph.D. dissertation, advisor: M. R. von Spakovsky, Virginia Polytechnic Institute and State University, February.

Rancruel, D. F., von Spakovsky, M. R., 2004, "Investigation of the Control Strategy Development Using an Integrated Model of a SOFC Based APU under Transient Conditions," *International Mechanical Engineering Congress and Exposition – IMECE'2004*, ASME Paper No. 62372, N.Y., N.Y., November.

Rancruel, D. F., von Spakovsky, M. R., 2005, "Development and Application of a Dynamic Decomposition Strategy for the Optimal Synthesis/Design and Operational/Control of a SOFC Based APU under Transient Conditions," *International Mechanical Engineering Congress and Exposition – IMECE'2005*, ASME Paper No. IMECE2005-82986, N.Y., N.Y., November.

Shah, R. S., 1981, "Compact Heat Exchanger Design Procedure", in Kakaç, S., Bergles, A. E., and Mayinger, F. (Editors), *Heat Exchangers, Thermal-Hydraulic Fundamentals and Design*, Hemisphere Publishing Corporation, Washington, pp. 495-536.